

Compartmental epidemic model to assess undocumented infections: applications to SARS-CoV-2 epidemics in Brazil

Guilherme S. Costa ,¹ Wesley Cota ,¹ and Silvio C. Ferreira ,^{1,2}

¹Departamento de Física, Universidade Federal de Viçosa, 36570-900 Viçosa, Minas Gerais, Brazil

²National Institute of Science and Technology for Complex Systems, 22290-180, Rio de Janeiro, Brazil

Nowcasting and forecasting of epidemic spreading, fundamental support for policy makers' decisions, rely on incidence series of reported cases to derive the fundamental epidemiological parameters. Two relevant drawbacks for predictions are the unknown fraction of undocumented cases and levels of nonpharmacological interventions that span highly heterogeneously across different places. We describe a simple approach using a compartmental model including asymptomatic and pre-asymptomatic contagions that allows to estimate both the level of undocumented infections and the value of R_t from reported case series in terms of epidemiological parameters. The method was applied to epidemic series for of COVID-19 across different municipalities in Brazil allowing to quantify the heterogeneity level of under-reporting across different places. The reproductive number derived within the current framework is little sensitive to both diagnosis and infection rates during the asymptomatic states, while being very sensitive to variations in case count series. The methods described here are general and we expect that they can be extended to other epidemiological approaches and surveillance data.

I. INTRODUCTION

Our contemporary society is facing an unprecedented threat imposed by the COVID-19, caused by the pathogen SARS-CoV-2, evidencing the importance, limitations, and subtleties of using compartmental epidemic models for the forecasting or even the nowcasting of pandemic scenarios [1–5]. After two years of intensive investigation, much has been learned with respect to the virology of SARS-CoV-2 in humans [6–9], several key aspects of the transmission were unveiled [5, 10–12], and efficient vaccines have been developed [13], among other achievements. Variants of SARS-CoV-2 [14, 15] give rise to new and more aggressive outbreaks due to reinfection and raised contagion rates implying that natural herd immunity is definitely not an option [16]. The newest Omicron (B.1.1.529) variant [17], containing several mutations on genes of the spike proteins, a leading target of antibodies produced to combat a COVID-19 infection, emerges as a new concern. Whilst the biology of the virus and interaction with human hosts is better understood, other crucial aspects of the epidemiology, specially the behavioural ones, remains unpredictable even at a short-term, varying across time and location. In particular the non-pharmaceutical interventions (NPI), such as face masks, testing policies, and social distancing, have played a central role on spreading of COVID-19 [18–21]. The aforementioned NPIs contribute for reduction or increase of the effective contagion rate that, therefore, must be inferred from count case series via likelihood or other calibration methods [22, 23].

The most stringent epidemic characteristic of the SARS-CoV-2 contagion in humans is probably its high transmission before the onset of the symptoms [5, 11, 24], the presymptomatic individuals, and even for those that never manifest relevant symptoms [25, 26], the true asymptomatic individuals. The latter could be accessed

by mass testing and contact tracing, for example, practices defended by experts but rarely implemented. Seroprevalence studies for different phases and regions [14, 27] reveals population incidences of antibodies for SARS-CoV-2 in levels much higher than counts of COVID-19 cases reported in surveillance systems. So, the case fatality ratio (CFR), defined as the ratio between number of deaths and diagnosed cases, can differ substantially from the infection fatality ratio (IFR), defined as the fraction of all infections (documented or not) that evolves to death [27].

The level of under-reporting, in which the CFR is greater than the IFR, varies widely in different seroprevalence inquiries [27] due to several uncontrolled factors such as the testing policies (only symptomatic cases, contact tracing, etc.), availability (low or high income places), sensitivity (antigen or PCR), and seek for medical care, among others. The relation between seropositivity and immunity is not fully established and new emerging variants always opens path for reinfections and new outbreaks [28]. Therefore, to estimate the level of undocumented infections across different places and times remains a challenge. Epidemic models of statistical inference were developed to access the amount of undocumented infections of SARS-CoV-2. For example, Pullano et al. [29] estimated that 9 out 10 cases of symptomatic infections were not ascertained by the surveillance system in France from 11 May to 28 June 2020, suggesting that large numbers of symptomatic cases of COVID-19 did not seek for medical advice. Lu et al. [30] considered four complementary approaches to estimate the cumulative incidence of symptomatic cases of COVID-19 in the US and concluded that on April 4, 2020, the estimated case count was 5 to 50 times higher than the official positive test counts across the different states. Subramaniana et al. [31] used a model including testing information to fit the case and serology data from New York City to estimate a low proportion of symptomatic cases (13 to

18% of the total infections), and that the reproductive number could be larger than often assumed. Similarly, Irons and Raftery [32] used a similar approach to estimate that approximated 60% of the infection were not diagnosed by tests in USA as of March 7, 2021.

Due to the importance of asymptomatic or pre-symptomatic transmission, the corresponding compartments were soon included in mathematical models for COVID-19 [11, 33–36]. However, it is concomitantly an additional source of uncertainty in the initial conditions. Predictive scenarios of the first SARS-CoV-2 outbreak were either semi-quantitative [33, 37, 38] or based on Bayesian inference using reported cases' series [34, 39, 40]. Brazil is an example, certainly not an exception, of highly heterogeneous responses to COVID-19 pandemics due to the lack of coordinated policies across different administrative layers [41], in addition to the intrinsic variability of social-economic indexes across the country impacting directly the epidemiological outcomes. Therefore, a mechanistic approach for simulation of epidemic spreading with asymptomatic transmission calls for a systematic way to determine the initial conditions.

The contribution of asymptomatic infections and testing policies to the effective reproductive number R_t [42] through surveillance counts is an important issue [32]. The basic reproductive number is defined as the average number of secondary infections generated by a single infected individual introduced in a completely susceptible population, commonly represented by R_0 . The effective reproductive number is given by $R_t = S(t)R_0$, where S is the fraction of susceptible population (who can be infected) at time t . This definition, under the hypothesis of homogeneous mixing, is the simplest one and can be generalized to stratified compartments [42]. The reproductive number can also be estimated directly from case counts using statistical inference models [22], as commonly reported for COVID-19 pandemics across the world [19, 34, 41, 43].

In this present work, we describe an approach to estimate the number of undocumented cases (asymptomatic or not) using the epidemic surveillance data for cases and deaths. The method is grounded on a compartmental epidemic model including both documented and undocumented compartments (asymptomatic, exposed, symptomatic, and so on), the latter not counting for surveillance reports. The present approach allows to determine the effective reproductive number, the level of under-reporting, and initial condition using the day of diagnosis. The approach can be promptly modified or generalized for other types of data and epidemic compartments. The method shares similarities with the recent approaches to estimate undocumented cases [25, 29, 30, 32], such as the use of reported infections and deaths. The central difference is that our approach is more mechanistic and less Bayesian.

We applied the method across different geographical scales of two Brazilian states, namely Paraná (PR) and Espírito Santo (ES) using time series with dates of di-

agnosis of COVID-19 counts available by the epidemic surveillance of the respective states. The time windows of investigation was from 1 January to 31 May of 2021 corresponding to the second epidemic wave driven mainly by the Gamma variant [41, 44]. We observed variable levels of under-reporting across different places and times. Particularly, the analysis indicates that the fraction of undocumented cases is correlated positively with the epidemic incidence: the higher the epidemic incidence in case counts the larger the fraction of undocumented infections. We were able to estimate initial conditions for the hidden compartments and effective infection rates which gave an efficient short-time forecast for the series of confirmed cases. Despite the basic reproductive number being explicitly dependent on the asymptomatic transmission, the analysis indicates that undocumented infections seem to not alter significantly the reproductive number for the analyzed data.

The remaining of this paper is organized as follows. The methodology is detailed in section II. The epidemic compartmental model and some analytical results are presented in subsection II A. The data-driven approach to estimate the under-reporting level from surveillance counts is described in subsection II B while the eigenvalue approach to determine the initial conditions is presented in subsection II C. The application of method to epidemiological data is presented in section III and the main conclusions of the work are discussed in section IV.

II. SIMPLE APPROACH TO ESTIMATE UNDOCUMENTED CASES

A. Compartmental model

Presymptomatic, asymptomatic and undocumented transmissions are investigated using a compartmental model [42] under the homogeneous mixing hypothesis grouping individuals according to their epidemic states in the following compartments: *Susceptible* (S) who can be infected; *exposed* (E) who were infected but is not contagious yet; *asymptomatic* (A) who are infectious but do not present symptoms; *symptomatic* (I) ones who may seek for medical care and testing due to the presence of symptoms; *undocumented recovered* (R) who has been infected, healed but not diagnosed; *deceased* (D) who died due to COVID-19; two compartments of *diagnosed cases* for SARS-CoV-2 including individuals who were *asymptomatic* (C_A) or *symptomatic* (C_I) at moment of testing; and the corresponding *recovered compartments for confirmed cases* R_A and R_I . The epidemiological model and rates are schematically depicted in Fig. 1.

Susceptible persons in contact with infectious (asymptomatic or symptomatic) individuals become exposed with rates λ_A and λ_I , respectively. For sake of simplicity, confirmed cases are assumed to be isolated and do not contribute for new infections. The remaining transitions are spontaneous and expressed in Fig. 1. Exposed indi-

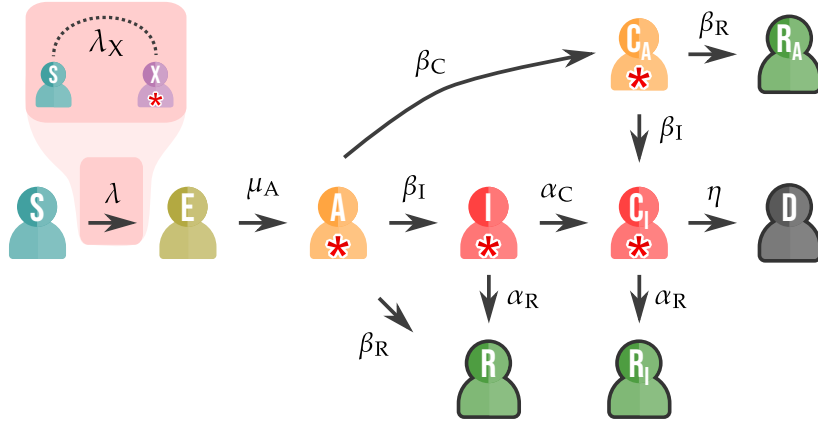


FIG. 1. Schematic representation of the epidemic model including the following compartments: susceptible (S), exposed (E), asymptomatic (A), symptomatic (I), recovered (R, R_A , and R_I), deceased (D), and confirmed cases (C_A and C_I). The transition and respective rates are indicated by arrows. The infectious compartments are depicted with the symbol \star . The infection processes, represented by the dashed line, involve the interaction between susceptible and one of the infectious compartments, happening with rates λ_X , $X=A, I, C_A$, and C_I , which can depend on the compartment.

viduals become asymptomatic with rate μ_A . The latter can evolve to a symptomatic state with rate β_I , recover with rate β_R , or be diagnosed by tests with rate β_C moving to the confirmed compartment C_A . Similarly, the undocumented symptomatic ones can recover with rate α_R or be diagnosed and become C_I with rate α_C . The clinical state of confirmed cases evolves as does the undocumented ones. An infected confirmed case (C_I) can die (D) with rate η while undocumented deaths are neglected, again, for sake of simplicity. The true asymptomatic and the presymptomatic cases are implicitly considered with transitions $A \rightarrow R$ ($C_A \rightarrow R_A$) and $A \rightarrow I$ ($A \rightarrow C_A \rightarrow C_I$), respectively. See Methods for the complete set of equations.

Consider a more intuitive parameterization in terms of the probabilities p_A and p_I that infected individuals are diagnosed during the asymptomatic or symptomatic phases, respectively, which can be computed from the compartmental model and are given by

$$p_A = \frac{\beta_C}{\beta_I + \beta_C + \beta_R} \quad \text{and} \quad p_I = \frac{\alpha_C}{\alpha_C + \alpha_R}. \quad (1)$$

One can also show that an exposed individual ends diagnosed with probability

$$\mathcal{P}_C = p_A + (1 - p_A)p_I\phi, \quad (2)$$

where $\phi = \beta_I/(\beta_I + \beta_R)$. The first and second terms of (2) are due to diagnosis during asymptomatic and symptomatic phases, respectively, while recovering without diagnosis happens with probability $\mathcal{P}_R = 1 - \mathcal{P}_C$. Therefore, we can determine a simple relation between the final number of documented (N_C) and undocumented (N_R) infections defining the under-reporting coefficient σ_{ur} as

$$\sigma_{ur} = \frac{N_R}{N_C} = \frac{\mathcal{P}_R}{\mathcal{P}_C} = \frac{(1 - p_A)(1 - \phi)p_I}{p_A + (1 - p_A)p_I\phi}, \quad (3)$$

where $N_C = N_{C_A} + N_{C_I} + N_{R_A} + N_{R_I} + N_D$.

We can also analytically determine the model's IFR ℓ_{IFR} , considering the probabilities that exposed individuals evolve to death passing through C_A compartment or not, that are $p_A \frac{\phi\eta}{\eta + \alpha_R}$ or $(1 - p_A)\phi p_I \frac{\eta}{\eta + \alpha_R}$, respectively. The IFR becomes

$$\ell_{IFR} = [p_A + (1 - p_A)p_I] \frac{\phi\eta}{\eta + \alpha_R}. \quad (4)$$

B. Estimating under-reporting from epidemic surveillance counts

The rates μ_A , β_I , β_R , α_R , and η are biological and can, in principle, be found in epidemiological surveys [6–9, 12, 45]. The parameters λ_A and λ_I depend on behavioral aspects such as the number of potential infectious contacts per unit of time [20, 34, 38]; prophylactic attitudes by means of NPI such as mask wearing and adoption of social distancing [46–48]; infectiousness and prevalence of new variants [14, 41, 49]; to cite only some of the most prominent issues. Similarly, the confirmation rates β_C and α_C depend on several behavioral and socioeconomic factors being highly influenced by testing policies [38, 50, 51]. All these aspects are very heterogeneously distributed across time and different places.

We describe how testing probabilities can be estimated from surveillance count series with the aid of the compartmental model of Figure 1. Let $\mathcal{C}(t)$ and $\mathcal{D}(t)$ represent the cumulative series of confirmed cases and deaths; and let x_A be the fraction of them which were confirmed during the asymptomatic stage. We equate the CFR computed for reported cases within a given time window $[t_{cal}, t_{cal} + \Delta\tau]$:

$$\ell_{CFR} \equiv \frac{\Delta\mathcal{D}(t_{cal})}{\Delta\mathcal{C}(t_{cal} - t_{delay})}, \quad (5)$$

and the CFR extracted from the model such that

$$\ell_{\text{CFR}} = \frac{\eta}{\eta + \alpha_R} x_A \phi + \frac{\eta}{\eta + \alpha_R} (1 - x_A), \quad (6)$$

in which t_{delay} is a delay between reported death and positive test report. The first and second terms in the right-hand side of (6) represent the probabilities of death for who were diagnosed for SARS-CoV-2 during the asymptomatic and symptomatic stages, respectively. Now, taking the ratio between Eqs. (4) and (5), one obtains

$$\frac{\ell_{\text{IFR}}}{\ell_{\text{CFR}}} = \frac{[p_A + (1 - p_A)p_I]\phi}{1 - x_A(1 - \phi)}. \quad (7)$$

Despite its simplicity, Eq. (7) is very handy since it relates the testing rates (or probabilities) with epidemiological parameters (ℓ_{IFR} and ϕ) or factors (x_A and ℓ_{CFR}) which could, in principle, be obtained directly from data. Therefore, if the ratio $r = p_A/p_I$ is given, the testing rates can be estimated.

We assume $r \leq 1$, that is, the chance of detecting asymptomatic is lower than of symptomatic cases. Equation (7) is therefore consistent ($p_A \leq p_I \leq 1$) only if

$$\zeta = [1 - x_A(1 - \phi)] \frac{\ell_{\text{IFR}}}{\ell_{\text{CFR}}} \leq \phi. \quad (8)$$

If inequality (8) is not satisfied, a value $p_I \lesssim 1$ ($\alpha_C \gg \alpha_R$) is fixed since $p_I = 1$ means instantaneous transition to the C_I compartment ($\alpha_C = \infty$) that implies numerical difficulties. The parameter x_A is not commonly available in epidemic surveillance data, which usually report only the total number of confirmed cases. However, we may assume $x_A \ll 1$ approximating the denominator of Eq. (7) by 1, for which we expect a small error in general. Also, a sensibility analysis of the ratio r can be used to verify whether the results are little sensitive to this choice (it was the case all data analyzed in this work); otherwise the ratio must be determined using some calibration or likelihood method.

C. Assessing hidden compartments from epidemic surveillance data

Epidemic surveillance provides the number of confirmed cases, deaths, date of first symptoms, or diagnosis; nothing with respect to the other compartments is commonly available. Actually, in the real scenario, the situation is much more complicated due to delays and other complex issues on surveillance counts [53, 54]. Using the case series $\mathcal{C}(t)$, we estimate infection rates λ_A and λ_I concomitantly with the initial conditions $(S^*, E^*, A^*, I^*, R^*)$ using the calibration procedure described in Methods Section A A 2. We applied the method to two types of count series available for Brazil, hereafter named Type-I and Type-II. The former consists of count series using release dates provided by epidemic surveil-

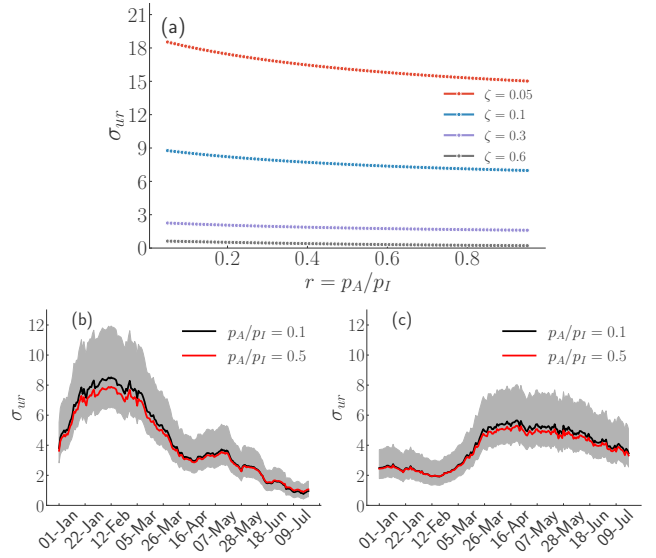


FIG. 2. (a) Under-reporting coefficient σ_{ur} as a function of p_A/p_I for different values of $\zeta = [1 - x_A(1 - \phi)] \frac{\ell_{\text{IFR}}}{\ell_{\text{CFR}}}$; see equation (8). Evolution of σ_{ur} for the capital cities of (b) Manaus and (c) São Paulo estimated using moving time windows of 3 weeks for type-I count series (see main text) as notified by state surveillance departments [52]. Two values of the ratio $p_A/p_I = 0.1$ and 0.5 were compared. The interval of confidence of is 95% shown in the shaded region.

lance departments of Brazilian federation units¹ which are aggregated and publicly available for all 5570 Brazilian municipalities [52]. These data do not yield the date of diagnosis and may present uncontrolled bias caused by reporting delays and should be used with care. The type-II data sets contain dates of diagnosis and first symptoms onset. In this work, we use the publicly available Type-II data for Paraná (PR) [55] and Espírito Santo (ES) [56] states. The data are publicly available in the cited resources and the data aggregated for different municipalities, used in the present work, is available on [57]. A full description of these datasets is available in the Supplementary Material (SM) [58].

We fixed the average values of parameters $\mu_A^{-1} = 3.2$ d and $\beta_I^{-1} = 3.2$ d so that the mean incubation time is of 6.4 d [6, 34]. The mean recovery time for symptomatic individuals was taken as $\alpha_R^{-1} = 3.2$ d [59]. Following [33, 34], asymptomatic cases were assumed to have the same recovering time such that $\beta_R^{-1} = \beta_I^{-1} + \alpha_R^{-1}$. Sensibility analysis was done drawing μ_A , β_I , and α_R from Gamma distributions with standard deviation of 1.3 d. The IFR ℓ_{IFR} was drawn from a uniform distribution in the range 0.5% to 1% in accordance with seroprevalence studies;

¹ Brazil is divided into 26 states and 1 federal district. States aggregate municipalities with independent administrative structure. Cases are reported by municipalities to state's healthcare departments which release the information publicly.

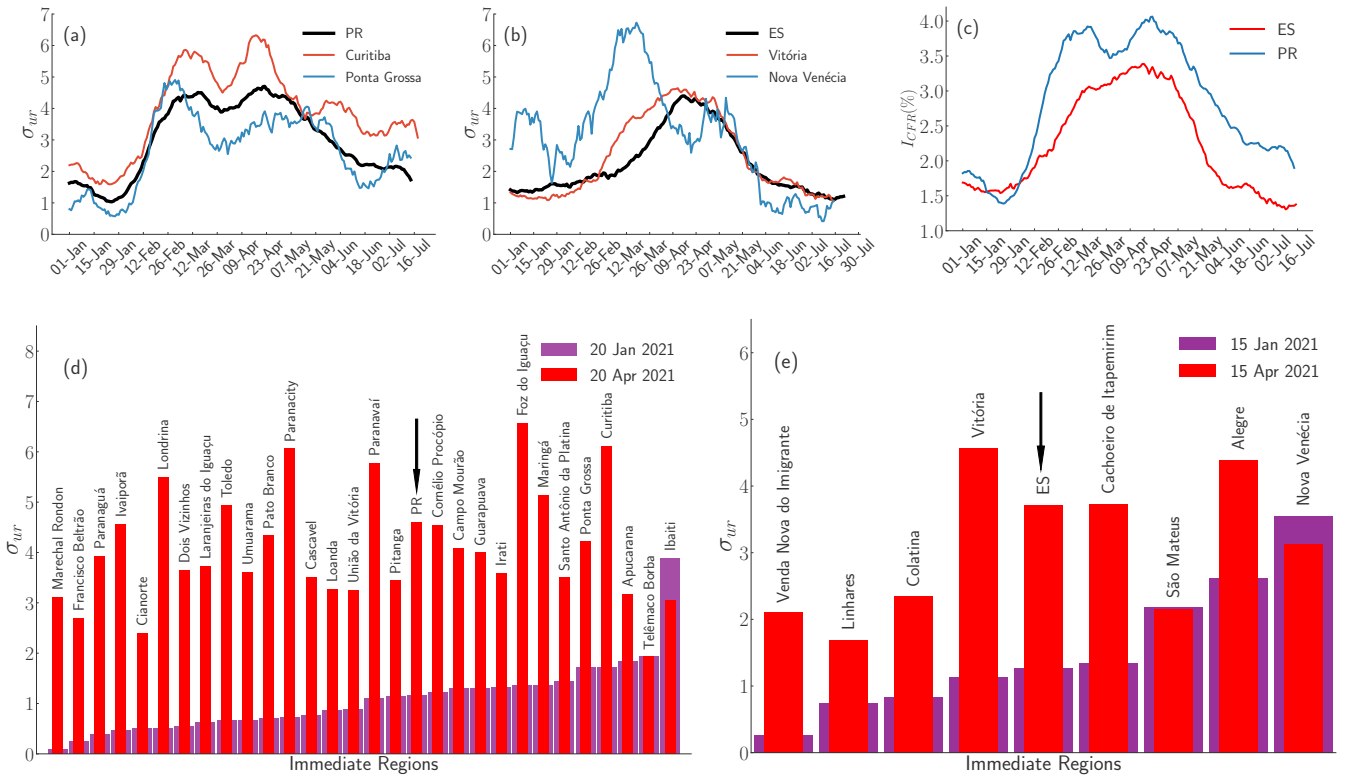


FIG. 3. Evolution of under-reporting coefficient for (a) PR and (b) ES states using $p_A/p_I = 0.1$ and time windows of 3 weeks. Two immediate regions of each state are presented in the corresponding panels. (c) Evolution of the CFR computed using delays $t_{\text{delay}} = 10$ d and 20 d for PR and ES states, respectively. Under-reporting coefficients for all immediate regions of (d) PR and (e) ES and the for states (indicated by arrows) computed when the CFR is low (Jan 2021) and high (April 2021).

See Ref. [27] for collection of reports up to September 2020. We analyzed case report series for PR state and found out a delay of $t_{\text{delay}} \approx 10$ d between death and positive test report. For ES state this delay was $t_{\text{delay}} \approx 20$ d. The delay is obtained by shifting the time series so that the peaks of deaths and cases coincide, as shown in Fig. S1 of the Supplementary Material (SM) [58]. We consider t_{tr} as January 1st 2021.

III. RESULTS

A. Under-reporting coefficient

The under-reporting coefficient σ_{ur} is little sensitive to the choice of ratio $r = p_A/p_I$ as shown in Fig 2(a). The evolution of σ_{ur} using $r = 0.1$ and 0.5 for Type-I count series of two capital cities of Brazil, which were severely impacted by COVID-19 second infection wave, namely Manaus and São Paulo [41], are presented in Figs. 2(b) and (c), for which the estimated delays between case and death confirmations were $t_{\text{delay}} = 7$ and 9 days, respectively; see Figs. S1 (a) and (b) in the SM [58]. The value of σ_{ur} is practically the same or both ratios with differences lying within a confidence interval of 95%. The ratio $r = 0.1$ is adopted in all results presented hereafter. The

values of σ_{ur} were higher when both cities were facing high epidemic incidence.

We analyzed Type-II count series for PR and ES states aggregating data of municipality level into immediate regions defined by the Instituto Brasileiro de Geografia e Estatística (IBGE) [60] as a group of nearby municipalities of a same state with intense interchange for immediate needs (purchasing, work, healthcare, education, and so on). The evolution of σ_{ur} since January 2021 computed with counts aggregated by states and two selected immediate regions are shown in Figures 3(a) and (b) for PR and ES, respectively. Curves for the 28 and 8 immediate regions of PR and ES, respectively, with the confidence intervals are available in Figs. S2 and S3 of the SM [58]. A strong correlation between σ_{ur} and the CFR is observed, Fig. 3(c), since Eqs. (7) and (3) imply $\sigma_{\text{ur}} \propto \ell_{\text{CFR}}$ for a fixed value of p_I . The second relevant outcome is the substantial variation of undocumented infection along the time and across different places. For example, in Nova Venécia-ES, σ_{ur} ranges from below 1 to higher than 6. The under-reporting coefficient for all immediate regions of both PR and ES states are presented in Figs. 3(d) and (e); the chosen dates correspond to low and high CFR in the respective state counts. The differences between immediate regions can be up to

3-fold in a same time interval. The space-time variability reflects the high diversities of outbreak across different places, due to unsynchronized and unequal responses to pandemics besides demographic, economic, and developmental heterogeneity of states as predicted [33] and later observed [41] for the first epidemic wave in Brazil.

B. Determination of the initial conditions

To exemplify the calibration method, we performed the analysis for case counts of the PR state shown in Fig. 4; see Fig. S4 on SM [58] for the ES state. We further simplified the analysis assuming the same infection rate for both asymptomatic and symptomatic individuals prior diagnosis confirmation, $\lambda_A = \lambda_I$, implying in a single parameter to fit the data. Typical calibration curves are presented in Fig. 4(a)-(i) for different times using a 14-day moving window of calibration. A forecast of 1 week is also presented to verify the calibration robustness, reproducing very well the short-term progression of the cumulative case count time series. The method also performs very well for smaller geographical scales such as immediate regions; Fig. S5 of the SM [58].

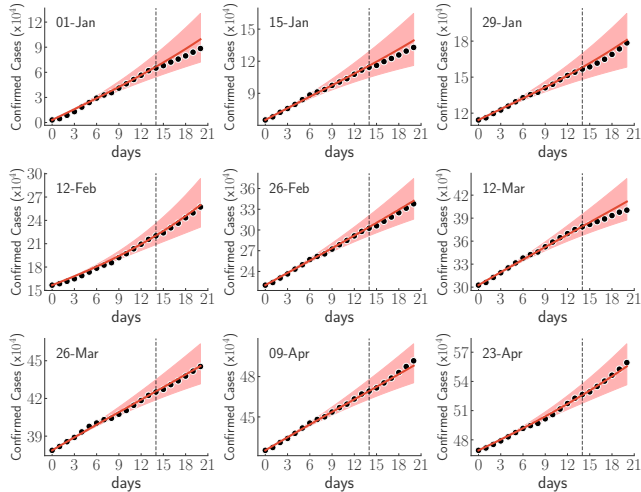


FIG. 4. Calibration curves for PR state in different time windows of 14 days indicated by the vertical lines. Initial day is in the top of each panel. One week of forecasting is also shown. Symbols are the cumulative cases' counts while lines with shaded regions represent the calibrated curves and the corresponding confidence interval of 95%.

The evolution of the undocumented epidemic compartments (exposed, asymptomatic, and symptomatic) yielded by the calibration method for PR state from January to May 2021 is presented in Fig. 5. Remark that the ratio between the total amount of infected individuals and the number of confirmed cases at a given day is much higher than the under-reporting coefficient shown in Fig. 3 since the latter refers to the final epidemic chain

where an infection ends documented or not, whereas the former refers to the amount of infected individuals in a given day which has not been documented yet. The peaks of prevalence of infectious cases happen slightly before peaks of incidence of confirmed cases. The effective reproduction number for PR state is presented in Fig. S6 on SM [58]. The calibration is sensitive to the variations and inflections in case count series, where the mean value of R_t oscillated between approximately 0.9 and 1.2. We performed a sensibility analysis of R_t and verified that its value is almost independent of the testing rates of asymptomatic compartments. More precisely, the curves of R_t collapses within the confidence interval when the ratios between testing probabilities p_A/p_I and infection rates λ_A/λ_I are varied by one order of magnitude.

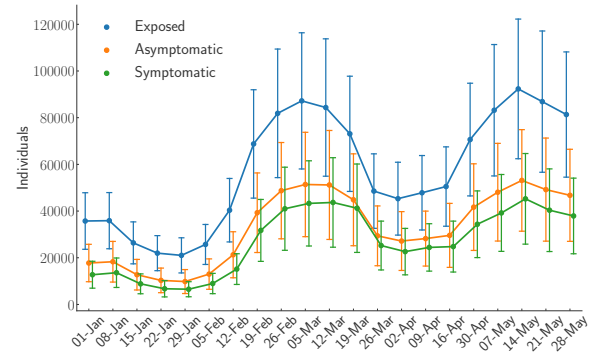


FIG. 5. Evolution of the undocumented compartments (exposed, asymptomatic and symptomatic) for the PR state since 1 January 2021.

IV. DISCUSSION

The pandemic caused by the SARS-CoV-2 led to unprecedented efforts gathering scientific community, epidemic surveillance, public authorities, and communication systems to provide almost real-time updated and publicly available counts for diagnosed infections, deaths, and other important statistics for COVID-19 spread across the globe. Available epidemic series, however, are still not ideal since under-reporting, delays, and many other issues intrinsic of our limited capacity in documenting are unavoidable. Moreover, these limitations vary enormously across different places and at different moments reflecting the unequal contemporary world, from socioeconomic to educational perspectives. However, this opens new avenues for construction and improvement of tools to extract information which are not explicit in data. A common strategy, possibly the gold standard in applied epidemiology, is the use of Bayesian inference models [29, 30]. A particularly promising strategy is the data-driven [33, 34, 37] approach where mathematical and mechanistic models are supplied by data, allowing to make predictions which are not explicitly avail-

able. In the case of COVID-19 we have the important class of asymptomatic or pre-symptomatic infections, in which individuals transmit the SARS-CoV-2 pathogen even without symptoms, being very difficult to be detected in epidemic surveillance systems.

In the present work we follow a data-driven approach using a compartmental model to estimate the amount of undocumented cases in the epidemic compartments which are not directly accessible in surveillance systems. The method allows to estimate the fraction of undocumented infections using case fatality ratio (CFR) and biological parameters estimated in controlled studies, in particular the infection fatality ratio (IFR). We applied the method to epidemic series of diagnosed cases and deaths of two Brazilian states where days of the symptoms onset were available. We selected the first semester of 2021 where Brazil was struck by a second epidemic wave of COVID-19, mainly driven by the Gamma variant (lineage P.1). We calculated a under-reporting coefficient σ_{ur} , giving the ratio between infections which ends diagnosed by tests or not. Our analysis reports a large variation of σ_{ur} , up to one order of magnitude, along the time and also across different locations at the same period. The method allows to estimate the initial condition for the undocumented compartments, in particular the asymptomatic and exposed ones. The undocumented symptomatic cases are estimated as being approximately 1/5 of all infected individuals in a given moment. While, on the one hand, these numbers should be not interpreted as accurate estimates of actual epidemic prevalence, on the other hand, they clearly demonstrate that the infected individuals that can potentially seek for medical assistance are a minor part of all cases. Interestingly, the effective reproduction number is almost insensitive to the testing rate of asymptomatic cases, confirming that undocumented infections do not affect this important epidemic indicator.

The method can be generalized for stratified data including age contact matrices [61] or metapopulation approaches [33, 34]. However, the main lesson is that initial conditions for undocumented compartments can be inferred using a simple mechanistic approach, based on compartmental models fueled by basic epidemic series of diagnosed death and cases. Nonetheless, the accuracy of methods depends on good estimates of biological parameters, mainly the IFR that changes as the epidemic scenario is altered. For example, vaccination is expected to reduce IFR while the emergence of more aggressive variants can increase it.

Appendix A: Methods

Here we describe the methods used to evolve the compartmental model and its calibration with real data.

1. Equations of the compartmental model

Assuming a constant population $N = \sum_X N_X$, where N_X is the number of individuals in the compartment X , the above transitions can be summarized in the following set of differential equations

$$\frac{dS}{dt} = -(\lambda_A A + \lambda_I I)S \quad (A1a)$$

$$\frac{dE}{dt} = (\lambda_A A + \lambda_I I)S - \mu_A E \quad (A1b)$$

$$\frac{dA}{dt} = \mu_A E - (\beta_I + \beta_R + \beta_C)A \quad (A1c)$$

$$\frac{dI}{dt} = \beta_I A - (\alpha_R + \alpha_C)I \quad (A1d)$$

$$\frac{dR}{dt} = \alpha_R I + \beta_R A \quad (A1e)$$

$$\frac{dC}{dt} = \beta_C A + \alpha_C I \quad (A1f)$$

$$\frac{dC_A}{dt} = \beta_C A - (\beta_R + \beta_I)C_A \quad (A1g)$$

$$\frac{dC_I}{dt} = \alpha_C I + \beta_I C_A - (\alpha_R + \eta)C_I \quad (A1h)$$

$$\frac{dR_A}{dt} = \beta_R C_A \quad (A1i)$$

$$\frac{dR_I}{dt} = \alpha_R C_I \quad (A1j)$$

$$\frac{dD}{dt} = \eta C_I, \quad (A1k)$$

where $X = N_X/N$, $X \in \{S, E, \dots, D\}$, is the corresponding population fraction in the compartment X .

The basic reproductive number R_0 is straightforwardly computed and given by

$$R_0 = \frac{1}{\beta_I + \beta_C + \beta_R} \left[\lambda_A + \lambda_I \frac{\beta_I}{\alpha_C + \alpha_R} \right]. \quad (A2)$$

2. Calibration procedure

In this section we describe the calibration procedure for the estimation of under-reporting from epidemic surveillance counts. The steps are the following:

- i. Select the time interval $[t_{\text{cal}}, t_{\text{cal}} + \Delta\tau]$ for which the reported case series $\mathcal{C}(t)$ will be analyzed. This time window should be short enough to assume that infection rates λ_A and λ_I are approximately constant, but sufficiently large to have significant amount of data;
- ii. Using the time series of case and death counts, determine the probability p_I using Eq. (7) for a given ratio $r = p_A/p_I$, assumed to be a parameter of the method. Determine the under-reporting coefficient given by Eq. (3).
- iii. Consider an adiabatic approximation assuming that susceptible population varies much more slowly than the other compartments such that one can neglect its variation and take $S(t) \approx S^*$ as being constant over the investigated period.
- iv. Start with guessed initial values for the products $\gamma_A = \lambda_A S^*$ and $\gamma_I = \lambda_I S^*$ (to be fitted with data).
- v. Determine the number of undocumented cases N_R^* at $t = t_{\text{cal}}$ using the under-reporting coefficient calculated in step (ii) and the number of confirmed cases $N_C^* = \mathcal{C}(t_{\text{cal}}) - \mathcal{C}(t_{\text{tr}})$ from case counting, where t_{tr} is a transient time.
- vi. Under these conditions the compartmental model provides a closed linear system $\dot{\mathbf{X}} = \mathbb{J}\mathbf{X}$ for the infectious compartments $\mathbf{X} = (E, A, I)$ where the Jacobian is given by

$$\mathbb{J} = \begin{bmatrix} -\mu_A & \gamma_A & \gamma_I \\ \mu_A & -(\beta_I + \beta_R + \beta_C) & 0 \\ 0 & \beta_I & -(\alpha_R + \alpha_C) \end{bmatrix}. \quad (\text{A3})$$

We assume that the solution is ruled by the leading term $\mathbf{X} \sim \mathbf{v}_1 \exp[\Lambda_1(t - t_{\text{cal}})]$ where $\mathbf{v}_1 = (v_E, v_A, v_I)$ is the principal eigenvector corresponding to the largest eigenvalue Λ_1 of \mathbb{J} , providing two relation among initial conditions (E^*, A^*, I^*)

$$\frac{E^*}{A^*} \approx \frac{v_E}{v_A}, \quad (\text{A4})$$

$$\frac{I^*}{A^*} \approx \frac{v_I}{v_A}. \quad (\text{A5})$$

Using again $\mathbf{X} \sim \mathbf{v}_1 \exp[\Lambda_1(t - t_{\text{cal}})]$, a closed system of initial conditions for (E^*, A^*, I^*) is obtained with the integration of Eq. (A1f)

$$\Delta\mathcal{C} \approx (\beta_C A^* + \alpha_C I^*) \frac{e^{\Lambda_1 \Delta\tau} - 1}{\Lambda_1}, \quad (\text{A6})$$

where $\Delta\mathcal{C}$ is the increment of confirmed cases during the interval $\Delta\tau$ which is given by the reported case counts. If $\Lambda_1 \Delta\tau \ll 1$ we obtain

$$\beta_C A^* + \alpha_C I^* \approx \frac{\Delta\mathcal{C}}{\Delta\tau}. \quad (\text{A7})$$

Finally, the susceptible population is determined as

$$N_S^* = N - \sum_{X \neq S} N_X, \quad (\text{A8})$$

$S^* = N_S/N$, and the infection rates self-consistently estimated as $\lambda_A = \gamma_A/S^*$ and $\lambda_I = \gamma_I/S^*$.

- vii. Equations (A1b) to (A1f) are integrated in the interval $[t_{\text{cal}}, t_{\text{cal}} + \Delta\tau]$ and the dispersion with respect to the case counts is computed as $\Omega(\gamma_I, \gamma_A) = \|\mathcal{C} - C\|$.
- viii. The parameters γ_A and γ_I are incremented interactively and steps (iv) to (vii) are implemented using a multi-parametric bisection method to minimize $\Omega(\gamma_I, \gamma_A)$.

We remark that new variants and waning immunity lead to reinfections such that individuals recovered from an infection can still be susceptible, justifying to discard of cases before the transient time t_{tr} . Another source of uncertainty is the vaccination which also confers unknown levels of immunity to infections affecting directly the susceptible population. Vaccination will impact both the IFR and CFR, such that the update values of the IFR should be considered.

Code and data: Fortran and Python codes used for calibration and processing the epidemic series were made publicly in [57]. A description of the datasets and codes can be found in the SM [58].

Author contributions: GSC wrote the codes and performed the numerical studies. WC collected epidemic data. GSC, WC, and SCF conceived the method. SCF wrote the first version of the manuscript. All authors edited the manuscript and analyzed the results.

Competing interests: Authors declare no competing interest.

ACKNOWLEDGMENTS

This work was partially supported by the Brazilian agencies *Coordenação de Aperfeiçoamento de Pessoal de Nível Superior* - CAPES (Grant no. 88887.507046/2020-00), *Conselho Nacional de Desenvolvimento Científico e Tecnológico* - CNPq (Grants no. 430768/2018-4 and 311183/2019-0) and *Fundação de Amparo à Pesquisa do Estado de Minas Gerais* - FAPEMIG (Grant no. APQ-02393-18). This study was financed in part by the *Coordenação de Aperfeiçoamento de Pessoal de Nível Superior* (CAPES) - Brasil - Finance Code 001.

[1] J. T. Wu, K. Leung, and G. M. Leung, *Lancet* **395**, 689 (2020).

[2] J. Zhang, M. Litvinova, Y. Liang, Y. Wang, W. Wang, S. Zhao, Q. Wu, S. Merler, C. Viboud, A. Vespignani, M. Ajelli, and H. Yu, *Science* **368**, 1481 (2020).

[3] E. Estrada, *Phys. Rep.* **869**, 1 (2020).

[4] M. Gilbert, G. Pullano, F. Pinotti, E. Valdano, C. Poletto, P.-Y. Boëlle, E. D'Ortenzio, Y. Yazdanpanah, S. P. Eholie, M. Altmann, B. Gutierrez, M. U. G. Kraemer, and V. Colizza, *Lancet* **395**, 871 (2020).

[5] R. Li, S. Pei, B. Chen, Y. Song, T. Zhang, W. Yang, and J. Shaman, *Science* **368**, 489 (2020).

[6] Q. Li, X. Guan, P. Wu, X. Wang, L. Zhou, Y. Tong, R. Ren, K. S. Leung, E. H. Lau, J. Y. Wong, X. Xing, N. Xiang, Y. Wu, C. Li, Q. Chen, D. Li, T. Liu, J. Zhao, M. Liu, W. Tu, C. Chen, L. Jin, R. Yang, Q. Wang, S. Zhou, R. Wang, H. Liu, Y. Luo, Y. Liu, G. Shao, H. Li, Z. Tao, Y. Yang, Z. Deng, B. Liu, Z. Ma, Y. Zhang, G. Shi, T. T. Lam, J. T. Wu, G. F. Gao, B. J. Cowling, B. Yang, G. M. Leung, and Z. Feng, *N. Engl. J. Med.* **382**, 1199 (2020).

[7] H. Nishiura, N. M. Linton, and A. R. Akhmetzhanov, *Int. J. Infect. Dis.* **93**, 284 (2020).

[8] D. Baud, X. Qi, K. Nielsen-Saines, D. Musso, L. Pomar, and G. Favre, *Lancet Infect. Dis.* **20**, 773 (2020).

[9] X. He, E. H. Y. Lau, P. Wu, X. Deng, J. Wang, X. Hao, Y. C. Lau, J. Y. Wong, Y. Guan, X. Tan, X. Mo, Y. Chen, B. Liao, W. Chen, F. Hu, Q. Zhang, M. Zhong, Y. Wu, L. Zhao, F. Zhang, B. J. Cowling, F. Li, and G. M. Leung, *Nat. Med.* **26**, 672 (2020).

[10] L. C. Tindale, J. E. Stockdale, M. Coombe, E. S. Garlock, W. Y. V. Lau, M. Saraswat, L. Zhang, D. Chen, J. Wallinga, and C. Colijn, *eLife* **9**, 2020.03.03.20029983 (2020).

[11] J. C. Emery, T. W. Russell, Y. Liu, J. Hellewell, C. A. Pearson, K. E. Atkins, P. Klepac, A. Endo, C. I. Jarvis, N. G. Davies, E. M. Rees, S. R. Meakin, A. Rosello, K. van Zandvoort, J. D. Munday, W. J. Edmunds, T. Jombart, M. Auzenbergs, E. S. Nightingale, M. Jit, S. Abbott, D. Simons, N. I. Bosse, Q. J. Leclerc, S. R. Procter, C. J. Villabona-Arenas, D. C. Tully, A. K. Deol, F. Y. Sun, S. Hué, A. M. Foss, K. Prem, G. Medley, A. Gimma, R. Lowe, S. Clifford, M. Quaife, C. Diamond, H. P. Gibbs, B. J. Quilty, K. O'Reilly, G. M. Knight, R. M. Eggo, A. J. Kucharski, S. Funk, S. Flasche, and R. M. Houben, *eLife* **9**, 1 (2020).

[12] N. G. Davies, P. Klepac, Y. Liu, K. Prem, M. Jit, and R. M. Eggo, *Nat. Med.* **26**, 1205 (2020).

[13] M. Lipsitch and N. E. Dean, *Science* **370**, 763 (2020).

[14] N. G. Davies, S. Abbott, R. C. Barnard, C. I. Jarvis, A. J. Kucharski, J. D. Munday, C. A. B. Pearson, T. W. Russell, D. C. Tully, A. D. Washburne, T. Wenseleers, A. Gimma, W. Waites, K. L. M. Wong, K. van Zandvoort, J. D. Silverman, K. Diaz-Ordaz, R. Keogh, R. M. Eggo, S. Funk, M. Jit, K. E. Atkins, and W. J. Edmunds, *Science* **372**, eabg3055 (2021).

[15] L. F. Buss, C. A. Prete, C. M. M. Abraham, A. Mendrone, T. Salomon, C. de Almeida-Neto, R. F. O. França, M. C. Belotti, M. P. S. S. Carvalho, A. G. Costa, M. A. E. Crispim, S. C. Ferreira, N. A. Fraiji, S. Gurzenda, C. Whittaker, L. T. Kamaura, P. L. Takecian, P. da Silva Peixoto, M. K. Oikawa, A. S. Nishiya, V. Rocha, N. A. Salles, A. A. de Souza Santos, M. A. da Silva, B. Custer, K. V. Parag, M. Barral-Netto, M. U. G. Kraemer, R. H. M. Pereira, O. G. Pybus, M. P. Busch, M. C. Castro, C. Dye, V. H. Nascimento, N. R. Faria, and E. C. Sabino, *Science* **371**, 288 (2020).

[16] D. Sridhar and D. Gurdasani, *Science* **371**, 230 (2021).

[17] W. H. O. (WHO), (2021), classification of Omicron (B.1.1.529): SARS-CoV-2 Variant of Concern.

[18] A. Pan, L. Liu, C. Wang, H. Guo, X. Hao, Q. Wang, J. Huang, N. He, H. Yu, X. Lin, S. Wei, and T. Wu, *JAMA* **323**, 1915 (2020).

[19] S. T. Ali, L. Wang, E. H. Y. Lau, X.-K. Xu, Z. Du, Y. Wu, G. M. Leung, and B. J. Cowling, *Science* **369**, 1106 (2020).

[20] A. Goyal, D. B. Reeves, E. F. Cardozo-Ojeda, J. T. Schiffer, and B. T. Mayer, *eLife* **10** (2021), 10.7554/elife.63537.

[21] S. Flaxman, S. Mishra, A. Gandy, H. J. T. Unwin, T. A. Mellan, H. Coupland, C. Whittaker, H. Zhu, T. Berah, J. W. Eaton, M. Monod, P. N. Perez-Guzman, N. Schmit, L. Cilloni, K. E. C. Ainslie, M. Baguelin, A. Boonyasiri, O. Boyd, L. Cattarino, L. V. Cooper, Z. Cucunubá, G. Cuomo-Dannenburg, A. Dighe, B. Djaafara, I. Dorigatti, S. L. van Elsland, R. G. FitzJohn, K. A. M. Gaythorpe, L. Geidelberg, N. C. Grassly, W. D. Green, T. Hallett, A. Hamlet, W. Hinsley, B. Jeffrey, E. Knock, D. J. Laydon, G. Nedjati-Gilani, P. Nouvellet, K. V. Parag, I. Siveroni, H. A. Thompson, R. Verity, E. Volz, C. E. Walters, H. Wang, Y. Wang, O. J. Watson, P. Winskill, X. Xi, P. G. T. Walker, A. C. Ghani, C. A. Donnelly, S. Riley, M. A. C. Vollmer, N. M. Ferguson, L. C. Okell, and S. Bhatt, *Nature* **584**, 257 (2020).

[22] A. Cori, N. M. Ferguson, C. Fraser, and S. Cauchemez, *Am. J. Epidemiol.* **178**, 1505 (2013).

[23] K. M. Gostic, L. McGough, E. B. Baskerville, S. Abbott, K. Joshi, C. Tedijanto, R. Kahn, R. Niehus, J. A. Hay, P. M. De Salazar, J. Hellewell, S. Meakin, J. D. Munday, N. I. Bosse, K. Sherrat, R. N. Thompson, L. F. White, J. S. Huisman, J. Scire, S. Bonhoeffer, T. Stadler, J. Wallinga, S. Funk, M. Lipsitch, and S. Cobey, *PLOS Comput. Biol.* **16**, e1008409 (2020).

[24] K. Mizumoto, K. Kagaya, A. Zarebski, and G. Chowell, *Eurosurveillance* **25** (2020), 10.2807/1560-7917.ES.2020.25.10.2000180.

[25] O. Byambasuren, M. Cardona, K. Bell, J. Clark, M.-L. McLaw, and P. Glasziou, *Off. J. Assoc. Med. Microbiol. Infect. Dis. Canada* **5**, 223 (2020).

[26] D. Buitrago-Garcia, D. Egli-Gany, M. J. Counotte, S. Hossmann, H. Imeri, A. M. Ipekci, G. Salanti, and N. Low, *PLoS Med.* **17**, 1 (2020).

[27] J. P. A. Ioannidis, *Bull. World Health Organ.* **99**, 19 (2021).

[28] C. M. Romano, A. C. Felix, A. V. de Paula, J. G. de Jesus, P. S. Andrade, D. Cândido, F. M. de Oliveira, A. C. Ribeiro, F. C. da Silva, M. Inemami, A. A. Costa, C. O. de Leal, W. M. Figueiredo, C. S. Pannuti, W. M. de Souza, N. R. Faria, and E. C. Sabino, *Rev. Inst. Med. Trop. Sao Paulo* **63**, 0 (2021).

[29] G. Pullano, L. Di Domenico, C. E. Sabbatini, E. Valdano, C. Turbelin, M. Debin, C. Guerrisi, C. Kengne-

Kuetche, C. Souty, T. Hanslik, T. Blanchon, P.-Y. Boëlle, J. Figoni, S. Vaux, C. Campèse, S. Bernard-Stoecklin, and V. Colizza, *Nature* **590**, 134 (2021).

[30] F. S. Lu, A. T. Nguyen, N. B. Link, M. Molina, J. T. Davis, M. Chinazzi, X. Xiong, A. Vespignani, M. Lipsitch, and M. Santillana, *PLOS Comput. Biol.* **17**, e1008994 (2021).

[31] R. Subramanian, Q. He, and M. Pascual, *Proc. Natl. Acad. Sci.* **118**, e2019716118 (2021).

[32] N. J. Irons and A. E. Raftery, *Proc. Natl. Acad. Sci. U. S. A.* **118** (2021), 10.1073/pnas.2103272118.

[33] G. S. Costa, W. Cota, and S. C. Ferreira, *Phys. Rev. Res.* **2**, 043306 (2020), 2011.03380.

[34] A. Arenas, W. Cota, J. Gómez-Gardeñes, S. Gómez, C. Granell, J. T. Matamalas, D. Soriano-Paños, and B. Steinegger, *Phys. Rev. X* **10**, 041055 (2020).

[35] P. Ashcroft, S. Lehtinen, D. C. Angst, N. Low, and S. Bonhoeffer, *eLife* **10**, 1 (2021).

[36] L. Ferretti, C. Wymant, M. Kendall, L. Zhao, A. Nurtay, L. Abeler-Dörner, M. Parker, D. Bonsall, and C. Fraser, *Science* **368**, eabb6936 (2020).

[37] A. Aleta and Y. Moreno, *BMC Med.* **18**, 157 (2020).

[38] A. Aleta, D. Martín-Corral, A. Pastore y Piontti, M. Ajelli, M. Litvinova, M. Chinazzi, N. E. Dean, M. E. Halloran, I. M. Longini Jr, S. Merler, A. Pentland, A. Vespignani, E. Moro, and Y. Moreno, *Nat. Hum. Behav.* **4**, 964 (2020).

[39] J. Dehning, J. Zierenberg, F. P. Spitzner, M. Wibral, J. P. Neto, M. Wilczek, and V. Priesemann, *Science* **369**, eabb9789 (2020).

[40] B. F. Maier and D. Brockmann, *Science* **368**, 742 (2020).

[41] M. C. Castro, S. Kim, L. Barberia, A. F. Ribeiro, S. Gurzenda, K. B. Ribeiro, E. Abbott, J. Blossom, B. Rache, and B. H. Singer, *Science* **372**, 821 (2021).

[42] M. Keeling and P. Rohani, *Modeling Infectious Diseases in Humans and Animals* (Princeton University Press, 2008).

[43] N. M. Ferguson, D. Laydon, G. Nedjati-Gilani, N. Imai, K. Ainslie, M. Baguelin, S. Bhatia, A. Boonyasiri, Z. Cucunubá, G. Cuomo-Dannenburg, A. Dighe, I. Dorigatti, H. Fu, K. Gaythorpe, W. Green, A. Hamlet, W. Hinsley, L. C. Okell, S. Van Elsland, H. Thompson, R. Verity, E. Volz, H. Wang, Y. Wang, P. Gt Walker, C. Walters, P. Winskill, C. Whittaker, C. A. Donnelly, S. Riley, and A. C. Ghani, *Report 9: Impact of non-pharmaceutical interventions (NPIs) to reduce COVID19 mortality and healthcare demand*, Tech. Rep. March (2020).

[44] E. C. Sabino, L. F. Buss, M. P. S. Carvalho, C. A. Prete, M. A. E. Crispim, N. A. Frajji, R. H. M. Pereira, K. V. Parag, P. da Silva Peixoto, M. U. G. Kraemer, M. K. Oikawa, T. Salomon, Z. M. Cucunuba, M. C. Castro, A. A. de Souza Santos, V. H. Nascimento, H. S. Pereira, N. M. Ferguson, O. G. Pybus, A. Kucharski, M. P. Busch, C. Dye, and N. R. Faria, *The Lancet* **397**, 452 (2021).

[45] S. A. Lauer, K. H. Grantz, Q. Bi, F. K. Jones, Q. Zheng, H. R. Meredith, A. S. Azman, N. G. Reich, and J. Lessler, *Ann. Intern. Med.* **172**, 577 (2020).

[46] D. S. Candido, I. M. Claro, J. G. de Jesus, W. M. Souza, F. R. R. Moreira, S. Dellicour, T. A. Mellan, L. du Plessis, R. H. M. Pereira, F. C. S. Sales, E. R. Manuli, J. Thézé, L. Almeida, M. T. Menezes, C. M. Voloch, M. J. Fumagalli, T. M. Coletti, C. A. M. da Silva, M. S. Ramundo, M. R. Amorim, H. H. Hoeltgebaum, S. Mishra, M. S. Gill, L. M. Carvalho, L. F. Buss, C. A. Prete, J. Ashworth, H. I. Nakaya, P. S. Peixoto, O. J. Brady, S. M. Nicholls, A. Tanuri, Á. D. Rossi, C. K. V. Braga, A. L. Gerber, A. P. de C. Guimarães, N. Gaburo, C. S. Alencar, A. C. S. Ferreira, C. X. Lima, J. E. Levi, C. Granato, G. M. Ferreira, R. S. Francisco, F. Granja, M. T. Garcia, M. L. Moretti, M. W. Perroud, T. M. P. P. Castiñeiras, C. S. Lazari, S. C. Hill, A. A. de Souza Santos, C. L. Simeoni, J. Forato, A. C. Sposito, A. Z. Schreiber, M. N. N. Santos, C. Z. de Sá, R. P. Souza, L. C. Resende-Moreira, M. M. Teixeira, J. Hubner, P. A. F. Leme, R. G. Moreira, M. L. Nogueira, N. M. Ferguson, S. F. Costa, J. L. Proenca-Modena, A. T. R. Vasconcelos, S. Bhatt, P. Lemey, C.-H. Wu, A. Rambaut, N. J. Loman, R. S. Aguiar, O. G. Pybus, E. C. Sabino, and N. R. F. and, *Science* **369**, 1255 (2020).

[47] S. Moore, E. M. Hill, M. J. Tildesley, L. Dyson, and M. J. Keeling, *Lancet Infect. Dis.* **21**, 793 (2021).

[48] L. Di Domenico, G. Pullano, C. E. Sabbatini, P.-Y. Boëlle, and V. Colizza, *BMC Med.* **18**, 240 (2020).

[49] K. Kupferschmidt and M. Wadman, *Science* **372**, 1375 (2021).

[50] F. Ahmed, N. Ahmed, C. Pissarides, and J. Stiglitz, *Lancet Public Heal.* **5**, e240 (2020).

[51] K. Sun, W. Wang, L. Gao, Y. Wang, K. Luo, L. Ren, Z. Zhan, X. Chen, S. Zhao, Y. Huang, Q. Sun, Z. Liu, M. Litvinova, A. Vespignani, M. Ajelli, C. Viboud, and H. Yu, *Science* **371**, eabe2424 (2021).

[52] W. Cota, *SciELOPreprints.362* (2020), 10.1590/SciELO-Preprints.362.

[53] L. S. Bastos, T. Economou, M. F. C. Gomes, D. A. M. Villela, F. C. Coelho, O. G. Cruz, O. Stoner, T. Bailey, and C. T. Codeço, *Stat. Med.* **38**, 4363 (2019).

[54] L. S. Bastos, R. P. Niquini, R. M. Lana, D. A. M. Villela, O. G. Cruz, F. C. Coelho, C. T. Codeço, and M. F. C. Gomes, *Cad. Saude Publica* **36** (2020), 10.1590/0102-311x00070120.

[55] G. do Estado do Paraná, (2021), Boletim - Informe Epidemiológico Coronavírus (COVID-19), <https://www.saude.pr.gov.br/Pagina/Coronavirus-COVID-19> [Online; accessed 08-Sep-2021].

[56] G. do Estado do Espírito Santo, (2021), COVID-19 - Painel COVID-19 - Estado do Espírito Santo, <https://coronavirus.es.gov.br/painel-covid-19-es> [Online; accessed 08-Sep-2021].

[57] “Codes and datasets are freely available at <https://github.com/ghscosta/covid19-cal>.”

[58] “Supplementary material,”.

[59] J. M. Read, J. R. E. Bridgen, D. A. T. Cummings, A. Ho, and C. P. Jewell, *Philos. Trans. R. Soc. B Biol. Sci.* **376**, 20200265 (2021).

[60] Instituto Brasileiro de Geografia e Estatística (IBGE), *Divisão Regional do Brasil em Regiões Geográficas Immediatas e Regiões Geográficas Intermediárias* (Instituto Brasileiro de Geografia e Estatística Rio de Janeiro, 2017).

[61] K. Prem, A. R. Cook, and M. Jit, *PLOS Comput. Biol.* **13**, e1005697 (2017).